Received: 13 October 2020 | Revised: 11 January 2021 | Accepted: 12 February 2021

DOI: 10.1002/adc2.69

SPECIAL ISSUE ARTICLE

WILEY

On practical solutions of series elastic actuator control in the context of active disturbance rejection

Jinfeng Chen | **Yu Hu** | **Zhiqiang Gao**

The Department of Electrical Engineering and Computer Science, Cleveland State University, Cleveland, Ohio, USA

Correspondence
Jinfeng Chen, 2121 Euclid Ave, FH 332, Cleveland, OH 44115, USA.
Email: cjfhbchina@aliyun.com

Abstract

In this paper, customized series elastic actuator (SEA) force and position control solutions are proposed to achieve high performance while keeping the bandwidth low. In the context of active disturbance rejection, the higher the bandwidth of extended state observer, the more robust and accurate the closed-loop performance. However, high bandwidth requires high sampling frequency and low measurement noise, leading to higher cost in practice. It is shown in this paper that the bandwidth can be lowered without sacrificing performance by incorporating additional information into the design, including not only the entire known SEA model information but also angle measurements of both the motor and the load. In addition, this allows both matched and mismatched disturbances, at the motor and the load side respectively, to be estimated and mitigated in real time, thus making the design more robust. Simulation results verify the effectiveness and robustness of the proposed approach.

KEYWORDS

active disturbance rejection control (ADRC), motion control, series elastic actuator (SEA)

1 | INTRODUCTION

Series elastic actuator (SEA) is one of the most famous inherently compliant actuators in recent years, which has been widely used in physical human–robot interaction (pHRI) systems such as rehabilitation exoskeletons,[1-3] bionic prostheses,[4,5] and humanoids[6,7] since the first SEA was proposed by Pratt and Williamson in Reference 8. Unlike rigid actuators in traditional robot application, the SEA is developed by introducing an elastic element between a motor and a load. Even though increased stiffness can improve the precision, stability, and bandwidth of position control, SEA reducing stiffness provides a lot of advantages, such as shock absorption, passive compliance, improved energy efficiency, accurate and stable force control, and low mechanical output impedance.[9] These properties are important requirements for pHRI systems to intelligently interact with unstructured and dynamic environments.

SEA is challenging of its dynamics of two-mass-spring system, which can be considered as an equivalent system for a very common vibration system in industrial application such as vehicle suspension[10] and large optical telescope.[11] Therefore, the control of the SEA system is a conventional control problem in industry. This benchmark problem has been studied for a long time.[12-16] All these papers mainly focus on vibration suppression issues in two-mass-spring systems, which make compliant SEA more complicated than stiff actuators. Specifically, due to the interaction with unstructured and dynamic environments, the inertia and damping at the load side are rarely constant. An advanced controller should be designed to suppress vibration and perform well across a wide range of load inertia and damping. Moreover, external disturbance also can deteriorate the stability and performance.

In SEA, there are two kinds of control: force control and position control. In force control of the SEA, spring is utilized to transmit the force control problem to a position control problem (i.e., the adjustment of spring deflection between motor side and load side). Since it is impossible to accurately identify the dynamical parameters of load side and to measure the real-time interactive forces due to the interaction with unstructured and dynamic environment, it is difficult to design a high precision force control of SEA.[17-19] In order to obtain a high precision force control, a model-inverse time delay control was proposed in Reference 20 to compensate the uncertainties with almost no model information of motor and load sides and to decrease the influence of the delay between the desired and model dynamics by feedforwarding the inverse of desired model dynamics in time delay control. However, the time delay control is not a very good choice as mentioned in Reference 21. Although Reference 20 does not need any model information, the performance of force control may be improved by adding some known model information. Disturbance observer (DOB) force controllers proposed in References 22–24 add model information into the controller. However, the positions of motor side and load side both can be measured. They both can be added into the controller to improve control performance. A unified active disturbance rejection (ADR) motion controller, which applies disturbance rejection into state space, is proposed for position and force control problems of SEAs in References 25, 26. Its performance is limited by high observer bandwidth requirement and may deteriorate by low sampling frequency and high measurement noise in practice. Resonance ratio control combined with arm DOB is also applied to the force and position control problems of SEAs in Reference 27. However, its performance can be affected by variable disturbance due to the approximation of estimated disturbance fed back into reference input channel.

Although SEA has many advantages over conventional stiff actuators in force control, its position control problem is harder than that of the stiff actuators due to the elastic connection between a stiff actuator and a load. In SEA, the control input channel is different to the position output channel, which causes mismatched external disturbance. Then the load side of SEA is very sensitive to external disturbance, which can deteriorate the accuracy of position control. Different PD controllers combined with feed-forward are utilized in position control of SEA.[28,29] But it is difficult to tune PD gains, and model uncertainties and external disturbances are not considered in these papers. To improve the robustness, the position control in Reference 23 utilizes DOB force controller as a near idea force source to drive the output arm to follow the tracking trajectory. Reference 14 proposes a DOB position controller that directly uses motor torque as control input and gives a systematic and straightforward procedure to design Q-filter of DOB. However, it only can utilize one measurement at load side. Robust position control of SEA using backstepping with DOB is proposed in Reference 30, where the DOB is designed in the form of a second order high pass filter to estimate the matched and mismatched disturbances. However, its performance is also limited by high observer bandwidth requirement.

In this paper, a novel, customized active disturbance rejection control (ADRC) design is proposed for force and position control of SEAs, which can utilize not only known model information of motor side and load side but also two measurements including motor angle and load angle to lower the bandwidth requirement of extended state observer (ESO). In DOB-based controller design, the low observer bandwidth is crucial for practical application. Although high observer bandwidth increases robust and disturbance rejection, it also requires high sampling frequency and low measurement noise, which is a tradeoff in practical design. The new ADRC design proposed in this paper can greatly decrease the observer bandwidth requirement compared with Reference 25. Moreover, under the same observer bandwidth and control bandwidth, the performance of the proposed ADRC design is better than that of DOB in Reference 22.

In the proposed ADRC design, two output measurements are utilized. A matched disturbance and a mismatched disturbance in motor side and load side are estimated separately. Reference 31 uses a two-mass-spring system as an example and gives a detailed discuss about the relationship between total disturbance and multiple disturbances in a system with multiple disturbances. In practical design, more than one measurement can be measured, which means more measurement information can be utilized to controller design to improve robustness and performance. This paper proposes a new ADRC design incorporating multiple measurements. The simulation results have verified the improvement of robustness and performance.

Observability and controllability in the framework of modern control theory can be generalized to the systems with multiple disturbances and consider the disturbances as their states. Reference 32 considers the observability of the system with disturbances, while it assumes the lumped disturbances are constant. A necessary and sufficient condition of observability without assuming a constant disturbance is proposed in Reference 33. However, it only considers the situation which only includes a single lumped disturbance. This paper considers the observability of two disturbances in the motor side and load side and proposes a new ADRC design for motion control of SEAs. One of the two disturbances is a mismatched disturbance. Reference 34 proposes a disturbance compensation gain to counteract the mismatched disturbance

from the output channel. However, the disturbance compensation gain can be explained under the method of controllability in the framework of modern control theory. Then it is easier to derive the disturbance compensation gain. During the design of the proposed ADRC, we find that the observability and controllability considering disturbances as their states are very important concepts for ADRC design.

The remainder of the paper is organized as follows. In Section 2, the dynamic model of SEA is briefly introduced. Customized SEA force and position control solutions based on ADRC are proposed in Sections 3 and 4. In Section 5, the performance and robustness of the proposed ADRC are verified in simulations. A conclusion is given in Section 6.

2 | SEA DYNAMICS

Mechanical model of an SEA is shown in Figure 1. It includes four parts: a motor providing control input, a gear amplifying the output torque of the motor, a compliant component spring, and a load with an external torque applied on it. I_M and I_L represent the inertias of the motor and load, respectively; C_M and C_L represent the damping coefficients of the motor and load, respectively; the elasticity coefficient of load is K_L; N is the reduction ratio of the gear box; τ_M is the torque of driving motor; τ_L is the external torque applied on the load side; k is spring constant; θ_M is angular position of the motor side; and θ_L is the angular position of the load side. The contact of the SEA with environment can change the inertia, damping and elasticity of the load dynamics.[24] Due to the interaction with unstructured and dynamic environment, it is impossible to obtain accurate identification of load side parameters and measure the external torque applied on the load side in real time.

The dynamic equations of the SEA shown in Figure 1 are as follows:

$$(N^2 I_M s^2 + N^2 C_M s + k)\frac{\theta_M}{N} - k\theta_L = N\tau_M \tag{1}$$

$$(I_L s^2 + C_L s + K_L + k)\theta_L - k\frac{\theta_M}{N} = \tau_L \tag{2}$$

For force control, the spring between motor and load is utilized to convert the force control into position control. The output force is manipulated by the deflection of the spring. So, the output torque of the SEA is

$$\tau_d = k\left(\frac{\theta_M}{N} - \theta_L\right). \tag{3}$$

From (3), the reference position of the motor r can be derived to generate the reference output torque τ_d:

$$r = \left(\theta_L + \frac{\tau_d}{k}\right)N. \tag{4}$$

Then, the force controller of SEA is transformed into a position controller, where the motor tracks the reference trajectory in (4) in the presence of interactions with environment. For position control, the actuator's link at the load side should track the desired position trajectory with the control input at the motor side.

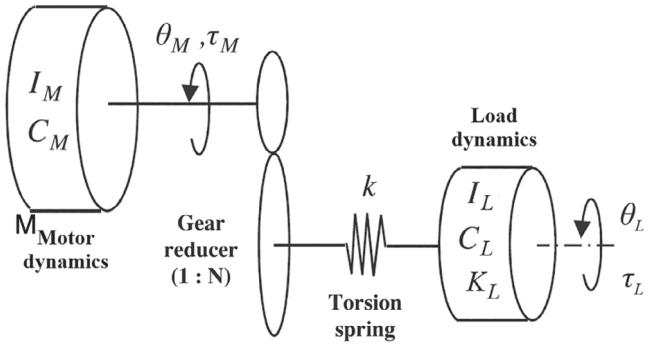

FIGURE 1 Model of SEA

3 | FORCE CONTROL OF SEAS

In this section, a conventional LADRC is introduced to force control of SEAs with no model information except the relative degree of the plant like the time delay control in Reference 20. In order to improve the performance, all known model information and two measurements are incorporated into LADRC design in the next subsection.

3.1 | LADRC without model information

In the framework of ADRC, the dynamical model of SEA can be rewritten as follows:

$$\ddot{\theta}_M = bu + f(\theta_M, u, d) \tag{5}$$

where θ_M is the output (i.e., motor position), u is the control input, d is the external disturbance, b is the control gain, and $f(\theta_M, u, d)$ is the total disturbance including model uncertainties and external disturbances of the plant. Since the relative degree of the plant is 2, (5) is a second-order differential equation. Therefore, there is no model information in (5) except for the relative degree of the plant. The control gain b should be tuned like the control distribution coefficient in Reference 20.

To estimate the total disturbance f in (5), an augmented variable is added into ordinary states.[35] The states in ESO are

$$x = \begin{bmatrix} \theta_M \\ \dot{\theta}_M \\ f \end{bmatrix}. \tag{6}$$

Assume f is differentiable. Equation (5) can be written in the form of state space

$$\begin{aligned} \dot{x} &= Ax + Bu + Eh \\ y &= Cx \end{aligned} \tag{7}$$

where $A = \begin{bmatrix} 0 & 1 & 0 \\ 0 & 0 & 1 \\ 0 & 0 & 0 \end{bmatrix}$, $B = \begin{bmatrix} 0 \\ b \\ 0 \end{bmatrix}$, $C = [1\ 0\ 0]$, $E = \begin{bmatrix} 0 \\ 0 \\ 1 \end{bmatrix}$, and $h = \dot{f}$.

A Luenberger state observer can be utilized to estimate all states as follows:

$$\begin{aligned} \dot{\hat{x}} &= A\hat{x} + Bu + L(y - \hat{y}) \\ \hat{y} &= C\hat{x} \end{aligned} \tag{8}$$

where $\hat{x} = \begin{bmatrix} \hat{x}_1 & \hat{x}_2 & \hat{x}_3 \end{bmatrix}^T$, L is the observer gain $L = \begin{bmatrix} \beta_1 & \beta_2 & \beta_3 \end{bmatrix}^T$. When the eigenvalues of $A - LC$ all have negative real parts, $\hat{x}_1$, $\hat{x}_2$, and $\hat{x}_3$ approximate θ_M, $\dot{\theta}_M$, and f, respectively. For the sake of simplicity of tuning, all the eigenvalues of $A - LC$ are placed at $-\omega_o$, which is the observer bandwidth.[36] Then, the observer gain is $L = \begin{bmatrix} 3\omega_0 & 3\omega_0^2 & \omega_0^3 \end{bmatrix}$. The estimated total disturbance can be subtracted from control input to be rejected. The control law is

$$u = \frac{-\hat{x}_3 + u_0}{b} \tag{9}$$

where u_0 is a close-loop control law such as PD controller. Substituting (9) into (5) yields

$$\ddot{\theta}_M = f(\theta_M, u, d) - \hat{x}_3 + u_0 \tag{10}$$

If the estimated total disturbance converges to f, the plant dynamical (5) becomes a simple second-order integral system

$$\ddot{\theta}_M = u_0. \tag{11}$$

In this section, the control law u_0 can be designated as

$$u_0 = k_1(r - \hat{x}_1) - k_2\hat{x}_2 \tag{12}$$

where r is the reference position of the motor in (4). k_1 and k_2 are control gains, which can be chosen as $k_1 = \omega_c^2$ and $k_2 = 2\omega_c$ by placing all the eigenvalues of (11) at $-\omega_c$, that is, the controller bandwidth.[36]

3.2 | LADRC with known model information and two measurements

A good mathematical model of the plant plays an important role in control design. The more model information added into control design, the better control performance you can have. Although it may be impossible to identify very accurate estimation of parameters of load dynamics due to the interaction with environment, some rough model information also can improve control performance. Therefore, in this section, nominal model of SEA and two measurements all are added into the control design to improve the observer performance.

In the dynamical equation of SEA shown in (1) and (2), there are two channels, which may both have a lumped disturbance applied on them,

$$(N^2 I_M s^2 + N^2 C_M s + k)\frac{\theta_M}{N} - k\theta_L = N\tau_M + f_1 \tag{13}$$

$$(I_L s^2 + C_L s + K_L + k)\theta_L - k\frac{\theta_M}{N} = f_2 \tag{14}$$

To design an observer with extended states to estimate lumped uncertainties f_1 and f_2, respectively, observable condition should be satisfied.[32] Since two lumped disturbances are included in different channels in SEA, two measurements, that is, motor angle and load angle, should be added in ESO to make the whole system observable. However, Reference 32 assumes that the lumped disturbances have constant values in steady state, that is, $\lim_{t\to\infty}\dot{f}(t) = 0$, which is impractical in real situation. To address this issue, a necessary and sufficient condition of design of an observer for uncertain nonlinear systems is proposed in Reference 33. However, it only considers the situation which only includes one output measurement. In SEA, there are two output measurements. In the following, the observability of SEA is discussed.

Equations (13) and (14) can be expressed in state space.

$$\begin{bmatrix}\dot{x}_1\\ \dot{x}_2\\ \dot{x}_3\\ \dot{x}_4\end{bmatrix} = A\begin{bmatrix}x_1\\ x_2\\ x_3\\ x_4\end{bmatrix} + B_u u + B_f\begin{bmatrix}f_1\\ f_2\end{bmatrix}$$
$$y = Cx \tag{15}$$

where $x_1 = \theta_M$, $x_2 = \theta_L$, $x_3 = \dot{\theta}_M$, $x_4 = \dot{\theta}_L$, $A = \begin{bmatrix}0 & 0 & 1 & 0\\ 0 & 0 & 0 & 1\\ -\frac{k}{N^2 I_M} & \frac{k}{N I_M} & -\frac{C_M}{I_M} & 0\\ \frac{k}{N I_L} & -\frac{K_L+k}{I_L} & 0 & -\frac{C_L}{I_L}\end{bmatrix}$, $B_u = \begin{bmatrix}0\\ 0\\ \frac{1}{I_M}\\ 0\end{bmatrix}$, $u = \tau_M$, $B_f = \begin{bmatrix}0 & 0\\ 0 & 0\\ 1 & 0\\ 0 & 1\end{bmatrix}$, $C = \begin{bmatrix}1 & 0 & 0 & 0\\ 0 & 1 & 0 & 0\end{bmatrix}$, $f_1 = f_1(x, d_1, t)$, $f_2 = f_2(x, d_2, t)$, d_1 is the external disturbance in channel 1, d_2 is the external disturbance in channel 2.

Adding two augmented state variables into ordinary state space, Equation (15) can be written as

$$\begin{bmatrix}\dot{x}\\ \dot{f}\end{bmatrix} = \begin{bmatrix}A & B_f\\ 0_{2\times 4} & 0_{2\times 2}\end{bmatrix}\begin{bmatrix}x\\ f\end{bmatrix} + \begin{bmatrix}B_u\\ 0_{2\times 1}\end{bmatrix}u + \begin{bmatrix}0_{4\times 2}\\ I_2\end{bmatrix}\dot{f}$$
$$y = \begin{bmatrix}C & 0_{2\times 2}\end{bmatrix}\begin{bmatrix}x\\ f\end{bmatrix} \tag{16}$$

where $x = \begin{bmatrix}x_1 & x_2 & x_3 & x_4\end{bmatrix}^T$, $f = \begin{bmatrix}f_1 & f_2\end{bmatrix}^T$, $0_{m\times n}$ is m by n zero matrix, I_n is n-dimension identity matrix. For the purpose of studying its observability, assume $u = 0$. By taking derivatives of the output equation of (16), the following equations can be obtained

$$y = \begin{bmatrix} C & 0_{2\times2} \end{bmatrix} \begin{bmatrix} x \\ f \end{bmatrix}$$
$$\dot{y} = \begin{bmatrix} CA & CB_f \end{bmatrix} \begin{bmatrix} x \\ f \end{bmatrix}$$
$$\ddot{y} = \begin{bmatrix} CA^2 & CAB_f \end{bmatrix} \begin{bmatrix} x \\ f \end{bmatrix} + CB_f\dot{f} \tag{17}$$

Putting Equation (17) in a matrix form yields

$$\begin{bmatrix} y \\ \dot{y} \\ \ddot{y} \end{bmatrix} = \begin{bmatrix} C & 0_{2\times2} \\ CA & CB_f \\ CA^2 & CAB_f \end{bmatrix} \begin{bmatrix} x \\ f \end{bmatrix} + \begin{bmatrix} 0_{2\times2} \\ 0_{2\times2} \\ CB_f \end{bmatrix} \dot{f} \tag{18}$$

From the theorem 2 in Reference 33, the necessary and sufficient condition of the observability of the above system is that (1) the matrix $\begin{bmatrix} C & 0_{2\times2} \\ CA & CB_f \\ CA^2 & CAB_f \end{bmatrix}$ is observable (full rank); (2) $\begin{bmatrix} 0_{2\times2} \\ 0_{2\times2} \\ CB_f \end{bmatrix}$ is a zero matrix; (3) the state x and the input u of system (15) are supposed to be bounded, and the external disturbances d_1 and d_2 and their one through forth-order derivatives are supposed to be bounded.

In order to verify whether the matrix $\begin{bmatrix} C & 0_{2\times2} \\ CA & CB_f \\ CA^2 & CAB_f \end{bmatrix}$ is observable, system matrix A, B_f, and C can be subdivided into a number of smaller submatrices $A = \begin{bmatrix} 0 & I_2 \\ A_{21} & A_{22} \end{bmatrix}$, $B_f = \begin{bmatrix} 0_{2\times2} \\ I_2 \end{bmatrix}$, $C = \begin{bmatrix} I_2 & 0_{2\times2} \end{bmatrix}$, respectively. Substituting them into observable matrix yields

$$\begin{bmatrix} C & 0_{2\times2} \\ CA & CB_f \\ CA^2 & CAB_f \end{bmatrix} = \begin{bmatrix} I_2 & 0 & 0 \\ 0 & I_2 & 0 \\ A_{21} & A_{22} & I_2 \end{bmatrix} \tag{19}$$

From (19), the observable matrix is full rank and observable. Moreover, $CB_f = \begin{bmatrix} I_2 & 0_{2\times2} \end{bmatrix} \begin{bmatrix} 0_{2\times2} \\ I_2 \end{bmatrix} = 0_{2\times2}$. So, the extended state system with two augmented state variables is observable. Therefore, a Luenberger state observer can be utilized to estimate all states. The corresponding ESO is

$$\begin{aligned} \dot{\hat{x}} &= \begin{bmatrix} A & B_f \\ 0_{2\times4} & 0_{2\times2} \end{bmatrix} \hat{x} + \begin{bmatrix} B_u \\ 0_{2\times1} \end{bmatrix} u + L(y - \hat{y}) \\ \hat{y} &= \begin{bmatrix} C & 0_{2\times2} \end{bmatrix} \hat{x} \end{aligned} \tag{20}$$

where $\hat{x} = \begin{bmatrix} \hat{x}_1 & \hat{x}_2 & \hat{x}_3 & \hat{x}_4 & \hat{x}_5 & \hat{x}_6 \end{bmatrix}^T$, L is the observer gain

$$L = \begin{bmatrix} \beta_{11} & \beta_{12} \\ \beta_{21} & \beta_{22} \\ \beta_{31} & \beta_{32} \\ \beta_{41} & \beta_{42} \\ \beta_{51} & \beta_{52} \\ \beta_{61} & \beta_{62} \end{bmatrix}. \tag{21}$$

Like the procedures in the above subsection, place all eigenvalues of (20) at $-\omega_o$. Thus, six simultaneous equations can be obtained, from which six unknown arguments can be solved. However, there are 12 unknown parameters in the observer gain L. So, we can assume the observe gain L is

$$L = \begin{bmatrix} \beta_{11} & 0 \\ 0 & \beta_{22} \\ \beta_{31} & 0 \\ 0 & \beta_{42} \\ \beta_{51} & 0 \\ 0 & \beta_{62} \end{bmatrix}. \tag{22}$$

Moreover, these six simultaneous equations are nonlinear. It is very difficult to have an analytic solution. The function vpasolve in Matlab can be used to obtain a numerical solution. Then $\hat{x}_1, \hat{x}_2, \hat{x}_3, \hat{x}_4, \hat{x}_5$, and $\hat{x}_6$ approximate $\theta_M, \theta_L, \dot{\theta}_M, \dot{\theta}_L, f_1$, and f_2, respectively. Therefore, the first channel in (13) can be uncoupled from the second channel in (14). Equation (13) can be written in the following form

$$\ddot{\theta}_M = -\frac{C_M}{I_M}\dot{\theta}_M - \frac{k}{N^2 I_M}\theta_M + \frac{k}{N I_M}\theta_H + \frac{1}{I_M}u + f_1 \tag{23}$$

Therefore, the control law is

$$u = \frac{\frac{k}{N^2 I_M}\hat{x}_1 - \frac{k}{N I_M}\hat{x}_2 + \frac{C_M}{I_M}\hat{x}_3 - \hat{x}_5 + u_0}{b} \tag{24}$$

where u_0 is a close-loop control law as in (12).

Remark 1. In (22), the zeros can be replaced by any constant values. It only changes the solution of observer gains. But the poles can always be placed at $-\omega_o$.

Remark 2. The Luenberger state observer in (20) is sixth order. In order to reduce the observer bandwidth further, this sixth order differential equation can be divided into two separate third order differential equations because θ_M and θ_L are both measurable outputs and both can be substituted into separate third order ESOs.

4 | POSITION CONTROL OF SEAS

LADRC can also be employed to position control of SEAs. The extension of LADRC with known model information proposed in References 37, 38 is introduced in the first subsection. The new LADRC design proposed in the previous section is capable of estimating matched and mismatched disturbances. Both disturbances are utilized in position control of SEAs in the second subsection.

4.1 | Extension of LADRC with known model information

Since the plant dynamics in LADRC takes the canonical form of cascade integrators, the dynamics of the SEA in (1) and (2) can be converted to a canonical form as follows:

$$\theta_L^{(4)} + \frac{C_L I_M + C_M I_L}{I_L I_M}\theta_L^{(3)} + \frac{(C_L C_M + I_M K_L + I_M k)N^2 + k I_L}{I_L I_M N^2}\ddot{\theta}_L + \frac{C_M(k + K_L)N^2 + k C_L}{I_L I_M N^2}\dot{\theta}_L + \frac{k K_L}{I_L I_M N^2}\theta_L = \frac{k}{I_L I_M N}u. \tag{25}$$

Adding a total disturbance on the right side of (25) and transforming it to state space form yield

$$\begin{aligned} \dot{x} &= Ax + Bu + Eh \\ y &= Cx \end{aligned} \tag{26}$$

where $A=\begin{bmatrix} 0 & 1 & 0 & 0 & 0 \\ 0 & 0 & 1 & 0 & 0 \\ 0 & 0 & 0 & 1 & 0 \\ -\frac{kK_L}{I_L I_M N^2} & -\frac{C_M(k+K_L)N^2+kC_L}{I_L I_M N^2} & -\frac{(C_L C_M+I_M K_L+I_M k)N^2+kI_L}{I_L I_M N^2} & -\frac{C_L I_M+C_M I_L}{I_L I_M} & 1 \\ 0 & 0 & 0 & 0 & 0 \end{bmatrix}$, $B=\begin{bmatrix} 0 \\ 0 \\ 0 \\ \frac{k}{I_L I_M N} \\ 0 \end{bmatrix}$, $E=\begin{bmatrix} 0 \\ 0 \\ 0 \\ 0 \\ 1 \end{bmatrix}$, $C=\begin{bmatrix} 1 & 0 & 0 & 0 & 0 \end{bmatrix}$, $x=\begin{bmatrix} \theta_L \\ \dot{\theta}_L \\ \ddot{\theta}_L \\ \theta_L^{(3)} \\ f \end{bmatrix}$.

Like the conventional LADRC, ESO can be designed by using Luenberger state observer

$$\begin{aligned} \dot{\hat{x}} &= A\hat{x} + Bu + L(y-\hat{y}) \\ \hat{y} &= C\hat{x} \end{aligned} \tag{27}$$

where $\hat{x}=\begin{bmatrix} \hat{x}_1 & \hat{x}_2 & \hat{x}_3 & \hat{x}_4 & \hat{x}_5 \end{bmatrix}^T$, L is the observer gain $L=\begin{bmatrix} \beta_1 & \beta_2 & \beta_3 & \beta_4 & \beta_5 \end{bmatrix}^{\mathrm{T}}$. Set all eigenvalues of $A-LC$ at $-\omega_o$, that is, solve $|\lambda I-(A-LC)|=(\lambda+\omega_o)^5$ for L. $\hat{x}_5$ is the estimation of total disturbance f, in which total disturbance includes all disturbances without known plant dynamics. Then the estimated total disturbance and the known plant dynamics can be subtracted from control input to be rejected. The control law is

$$u=\frac{\frac{kK_L}{I_L I_M N^2}\hat{x}_1+\frac{C_M(k+K_L)N^2+kC_L}{I_L I_M N^2}\hat{x}_2+\frac{(C_L C_M+I_M K_L+I_M k)N^2+kI_L}{I_L I_M N^2}\hat{x}_3+\frac{C_L I_M+C_M I_L}{I_L I_M}\hat{x}_4-\hat{x}_5+u_0}{b} \tag{28}$$

where u_0 is a close-loop control law designated as

$$u_0=k_1(r-\hat{x}_1)-k_2\hat{x}_2-k_3\hat{x}_3-k_4\hat{x}_4. \tag{29}$$

To place all the eigenvalues of the state-feedback control system at $-\omega_c$, the control gains are chosen as $k_1=\omega_c^4$, $k_2=4\omega_c^3$, $k_3=6\omega_c^2$ and $k_4=4\omega_c$.

4.2 | LADRC with known model information and two measurements

Since mismatched lumped disturbance f_2 at the load side is not in the control input channel, it can not be compensated from the control input channel directly. Moreover, no matter how the controller is designed, the mismatched disturbance cannot be removed completely from the system states. The influence of the mismatched disturbance can only be eliminated in output channel.[39] In the controllability theorem of modern control theory, it only studies the ability to transfer the dynamic system from any initial state to any desired final state. With mismatched and matched disturbances in the state space, we need to study the ability to transfer the dynamic system from any initial output to any desired final output. Like what the controllability theorem did, take the derivatives of the output equation, and every disturbance and control input all can be transformed to output channel. Then solve for the control input which can eliminate all mismatched and matched disturbances. The disturbance compensation gain proposed in Reference 34 can be extended to multiple disturbances and explained under the method of controllability as follows for position control of SEAs with two disturbances:

For position control, (13) and (14) can be expressed in state space:

$$\begin{aligned} \dot{x} &= Ax + B_u u + B_f f \\ y &= Cx \end{aligned} \tag{30}$$

where $x=\begin{bmatrix} \theta_M \\ \theta_L \\ \dot{\theta}_M \\ \dot{\theta}_L \end{bmatrix}$, $A=\begin{bmatrix} 0 & 0 & 1 & 0 \\ 0 & 0 & 0 & 1 \\ -\frac{k}{N^2 I_M} & \frac{k}{N I_M} & -\frac{C_M}{I_M} & 0 \\ \frac{k}{N I_L} & -\frac{K_L+k}{I_L} & 0 & -\frac{C_L}{I_L} \end{bmatrix}$, $B_u=\begin{bmatrix} 0 \\ 0 \\ \frac{1}{I_M} \\ 0 \end{bmatrix}$, $u=\tau_M$, $B_f=\begin{bmatrix} 0 & 0 \\ 0 & 0 \\ 1 & 0 \\ 0 & 1 \end{bmatrix}$, $f=\begin{bmatrix} f_1 \\ f_2 \end{bmatrix}$, $C=\begin{bmatrix} 0 & 1 & 0 & 0 \end{bmatrix}$, $f_1=f_1(x,d_1,t)$, $f_2=f_2(x,d_2,t)$, d_1 is the external disturbance in channel 1, d_2 is the external disturbance in channel 2.

From modern control theory,[40] state feedback is a linear combination of states. Since lumped disturbances are added to states, the assumed control law is

$$u = K_x\hat{x} + u_d(\hat{f}, \hat{\dot{f}}, \cdots, \hat{f}^{(k_d)}) \tag{31}$$

where $\hat{x}, \hat{f}, \cdots, \hat{f}^{(k_d)}$ are estimates of $x, f, \cdots, f^{(k_d)}$, respectively; k_d is a positive integer determined by plant dynamics; $K_x = \begin{bmatrix} k_1 & k_2 & k_3 & k_4 \end{bmatrix}$; u_d is a linear combination of lumped disturbances and their derivatives. To obtain analytic form of u_d, assume the above estimated values are their ideal values. Substituting (31) into (30) yields the close-loop system as

$$\begin{aligned} \dot{x} &= \overline{A}x + B_u u_d + B_f f \\ y &= Cx \end{aligned} \tag{32}$$

where $\overline{A} = A + B_u K_x$. After taking the fourth derivative of the output equation of (32), control input, output and disturbances all can be transformed into the output equation as follows:

$$y^{(4)} = C\overline{A}^4 x + \begin{bmatrix} C\overline{A}^3 B_u & C\overline{A}^2 B_u & C\overline{A}B_u & CB_u \end{bmatrix} \begin{bmatrix} u_d \\ \dot{u}_d \\ \ddot{u}_d \\ \dddot{u}_d \end{bmatrix} + \begin{bmatrix} C\overline{A}^3 B_f & C\overline{A}^2 B_f & C\overline{A}B_f & CB_f \end{bmatrix} \begin{bmatrix} f \\ \dot{f} \\ \ddot{f} \\ \dddot{f} \end{bmatrix} \tag{33}$$

Since the mismatched disturbance cannot be removed completely from the system state, the state x in (33) should be represented by the other variables in (33). Taking the first four derivatives of the output equation yields

$$\begin{bmatrix} y \\ \dot{y} \\ \ddot{y} \\ \dddot{y} \end{bmatrix} = \begin{bmatrix} C \\ C\overline{A} \\ C\overline{A}^2 \\ C\overline{A}^3 \end{bmatrix} x + \begin{bmatrix} 0 & 0 & 0 \\ CB_u & 0 & 0 \\ C\overline{A}B_u & CB_u & 0 \\ C\overline{A}^2 B_u & C\overline{A}B_u & CB_u \end{bmatrix} \begin{bmatrix} u_d \\ \dot{u}_d \\ \ddot{u}_d \end{bmatrix} + \begin{bmatrix} 0 & 0 & 0 \\ CB_f & 0 & 0 \\ C\overline{A}B_f & CB_f & 0 \\ C\overline{A}^2 B_f & C\overline{A}B_f & CB_f \end{bmatrix} \begin{bmatrix} f \\ \dot{f} \\ \ddot{f} \end{bmatrix} \tag{34}$$

Solving for x yields

$$x = \begin{bmatrix} C \\ C\overline{A} \\ C\overline{A}^2 \\ C\overline{A}^3 \end{bmatrix}^{-1} \begin{bmatrix} y \\ \dot{y} \\ \ddot{y} \\ \dddot{y} \end{bmatrix} - \begin{bmatrix} C \\ C\overline{A} \\ C\overline{A}^2 \\ C\overline{A}^3 \end{bmatrix}^{-1} \begin{bmatrix} 0 & 0 & 0 \\ CB_u & 0 & 0 \\ C\overline{A}B_u & CB_u & 0 \\ C\overline{A}^2 B_u & C\overline{A}B_u & CB_u \end{bmatrix} \begin{bmatrix} u_d \\ \dot{u}_d \\ \ddot{u}_d \end{bmatrix} - \begin{bmatrix} C \\ C\overline{A} \\ C\overline{A}^2 \\ C\overline{A}^3 \end{bmatrix}^{-1} \begin{bmatrix} 0 & 0 & 0 \\ CB_f & 0 & 0 \\ C\overline{A}B_f & CB_f & 0 \\ C\overline{A}^2 B_f & C\overline{A}B_f & CB_f \end{bmatrix} \begin{bmatrix} f \\ \dot{f} \\ \ddot{f} \end{bmatrix} \tag{35}$$

Substituting (35) into (33) yields

$$\begin{aligned} y^{(4)} = {} & C\overline{A}^4 \begin{bmatrix} C \\ C\overline{A} \\ C\overline{A}^2 \\ C\overline{A}^3 \end{bmatrix}^{-1} \begin{bmatrix} y \\ \dot{y} \\ \ddot{y} \\ \dddot{y} \end{bmatrix} + \left\{ \begin{bmatrix} C\overline{A}^3 B_u & C\overline{A}^2 B_u & C\overline{A}B_u & CB_u \end{bmatrix} - C\overline{A}^4 \begin{bmatrix} C \\ C\overline{A} \\ C\overline{A}^2 \\ C\overline{A}^3 \end{bmatrix}^{-1} \begin{bmatrix} 0 & 0 & 0 & 0 \\ CB_u & 0 & 0 & 0 \\ C\overline{A}B_u & CB_u & 0 & 0 \\ C\overline{A}^2 B_u & C\overline{A}B_u & CB_u & 0 \end{bmatrix} \right\} \begin{bmatrix} u_d \\ \dot{u}_d \\ \ddot{u}_d \\ \dddot{u}_d \end{bmatrix} \\ & + \left\{ \begin{bmatrix} C\overline{A}^3 B_f & C\overline{A}^2 B_f & C\overline{A}B_f & CB_f \end{bmatrix} - C\overline{A}^4 \begin{bmatrix} C \\ C\overline{A} \\ C\overline{A}^2 \\ C\overline{A}^3 \end{bmatrix}^{-1} \begin{bmatrix} 0 & 0 & 0 & 0 \\ CB_f & 0 & 0 & 0 \\ C\overline{A}B_f & CB_f & 0 & 0 \\ C\overline{A}^2 B_f & C\overline{A}B_f & CB_f & 0 \end{bmatrix} \right\} \begin{bmatrix} f \\ \dot{f} \\ \ddot{f} \\ \dddot{f} \end{bmatrix} \end{aligned} \tag{36}$$

If u_d can eliminate the disturbance f from the output y, the sum of the last two terms of right-hand side of (36) should be zero. Therefore, there is no disturbance terms in the output channel, which means the influence of disturbances have been compensated in the output channel. Substituting the parameters of SEA and solving for u_d yields a function including $f_1, f_2, \dot{f}_2$, and $\ddot{f}_2$. However, the ESO in the section 3.2 only can estimate f_1 and f_2. So, a new observer should be designed. From the idea of generalized proportional integral observer proposed in Reference 41, the new ESO can be designed. The states in the new ESO are $\begin{bmatrix} x & f_1 & f_2 & \dot{f}_2 & \ddot{f}_2 \end{bmatrix}^T$. Assume f_2 is third order differentiable. The extended state system can be written in the form of state space

$$\begin{bmatrix} \dot{x} \\ \dot{f}_1 \\ \dot{f}_2 \\ \ddot{f}_2 \\ \dddot{f}_2 \end{bmatrix} = \begin{bmatrix} A & B_d \\ 0_{4\times4} & B_e \end{bmatrix} \begin{bmatrix} x \\ f_1 \\ f_2 \\ \dot{f}_2 \\ \ddot{f}_2 \end{bmatrix} + \begin{bmatrix} B_u \\ 0_{4\times1} \end{bmatrix} u + \begin{bmatrix} 0_{4\times4} \\ E_h \end{bmatrix} \begin{bmatrix} \dot{f}_1 \\ \dot{f}_2 \\ \ddot{f}_2 \\ \dddot{f}_2 \end{bmatrix}$$
$$y = \begin{bmatrix} C & 0_{2\times4} \end{bmatrix} \begin{bmatrix} x \\ f_1 \\ f_2 \\ \dot{f}_2 \\ \ddot{f}_2 \end{bmatrix} \tag{37}$$

where $A = \begin{bmatrix} 0 & 0 & 1 & 0 \\ 0 & 0 & 0 & 1 \\ -\frac{k}{N^2 I_M} & \frac{k}{N I_M} & -\frac{C_M}{I_M} & 0 \\ \frac{k}{N I_L} & -\frac{K_L+k}{I_L} & 0 & -\frac{C_L}{I_L} \end{bmatrix}$, $B_d = \begin{bmatrix} 0 & 0 & 0 & 0 \\ 0 & 0 & 0 & 0 \\ 1 & 0 & 0 & 0 \\ 0 & 1 & 0 & 0 \end{bmatrix}$, $B_e = \begin{bmatrix} 0 & 0 & 0 & 0 \\ 0 & 0 & 1 & 0 \\ 0 & 0 & 0 & 1 \\ 0 & 0 & 0 & 0 \end{bmatrix}$, $B_u = \begin{bmatrix} 0 \\ 0 \\ \frac{1}{I_M} \\ 0 \end{bmatrix}$, $u = \tau_M$, $E_h = \begin{bmatrix} 1 & 0 & 0 & 0 \\ 0 & 0 & 0 & 0 \\ 0 & 0 & 0 & 0 \\ 0 & 0 & 0 & 1 \end{bmatrix}$, $C = \begin{bmatrix} 1 & 0 & 0 & 0 \\ 0 & 1 & 0 & 0 \end{bmatrix}$.

Then the corresponding ESO is

$$\begin{bmatrix} \dot{\hat{x}} \\ \dot{\hat{f}}_1 \\ \dot{\hat{f}}_2 \\ \ddot{\hat{f}}_2 \\ \dddot{\hat{f}}_2 \end{bmatrix} = \begin{bmatrix} A & B_d \\ 0_{4\times4} & B_e \end{bmatrix} \begin{bmatrix} \hat{x} \\ \hat{f}_1 \\ \hat{f}_2 \\ \dot{\hat{f}}_2 \\ \ddot{\hat{f}}_2 \end{bmatrix} + \begin{bmatrix} B_u \\ 0_{4\times1} \end{bmatrix} u + L(y - \hat{y})$$
$$\hat{y} = \begin{bmatrix} C & 0_{2\times4} \end{bmatrix} \begin{bmatrix} \hat{x} \\ \hat{f}_1 \\ \hat{f}_2 \\ \dot{\hat{f}}_2 \\ \ddot{\hat{f}}_2 \end{bmatrix} \tag{38}$$

where the observer gain is

$$L = \begin{bmatrix} \beta_{11} & 0 \\ 0 & \beta_{22} \\ \beta_{31} & 0 \\ 0 & \beta_{42} \\ \beta_{51} & 0 \\ 0 & \beta_{62} \\ 0 & \beta_{72} \\ 0 & \beta_{82} \end{bmatrix}. \tag{39}$$

The above observer gain can be numerically solved by Matlab function vpasolve such that all eigenvalues of characteristic matrix of (38) are placed at $-\omega_o$. Now every term in assumed control law in (31) is obtained except the control gain K_x. From (36), the original system with uncertainties can be considered as a nominal system after compensating uncertainties with u_d. Therefore, normal state-feedback pole placement can be utilized to determine control gain K_x. However, there exist steady-state errors if control law $u = r + K_x\hat{x} + u_d$ is used to track the reference r. The following method is based on reference input of state-feedback control[40] in the framework of model uncertainty and external disturbance.

Assume control input, output and states in steady state are u_{ss}, y_{ss} and x_{ss}, respectively. Since u_{ss} and x_{ss} are related to r_{ss} and the control law is (31), let

$$u_{ss} = N_u r_{ss} + u_d \tag{40}$$

$$x_{ss} = N_x r_{ss} \tag{41}$$

Substituting (40) and (41) into the steady state of (30) leads to

$$\dot{x}_{ss} = 0 = Ax_{ss} + B_u u_{ss} + B_f f = (AN_x + B_u N_u) r_{ss} + B_u u_d + B_f f \tag{42}$$

$$y_{ss} = r_{ss} = Cx_{ss} = CN_x r_{ss} \tag{43}$$

Since u_d is determined by canceling the influence of f from output, $B_u u_d + B_f f$ does not affect the output and then is equal to zero. So N_x and N_u can be solved from (42) and (43). In steady-state,

$$u - u_{ss} = K_x(x - x_{ss}) + u_d \tag{44}$$

Solving for u yields

$$u = (N_u - K_x N_x) r + K_x x + u_d \tag{45}$$

which is the control law with no steady-state errors.

5 | PERFORMANCE ANALYSIS BY SIMULATIONS

In order to verify the performances of the proposed ADRC with known model information and two output measurements, force and position control simulation results of an SEA are given in this section. The parameters of the whole dynamic plant model are given in Table 1, which are borrowed from Reference 24 to have a realistic simulation.

The force and position controllers of SEAs proposed in this paper are designed by using the following three steps.

Step 1. The state-feedback controller is a linear combination of plant states and lumped disturbances and their derivatives. First, the linear combination of plant states can be designed by pole placement neglecting internal and external disturbances. Second, the linear combination of lumped disturbances and their derivatives to eliminate matched and mismatched disturbances in the output channel can be designed by using controllability as in (36).

TABLE 1 Parameters of the plant in simulation

Parameter name	Symbol	Value
Motor inertia	I_M	5.2500e-6 kg m^2
Load inertia	I_L	0.0225 kg m^2
Motor damping	C_M	4.5356e-6 Nm s/rad
Load damping	C_L	0.4697 Nm s/rad
Environment spring stiffness	K_L	0.16 Nm/rad
Spring stiffness	k	0.48 Nm/rad
Gear reduction ratio	N	20

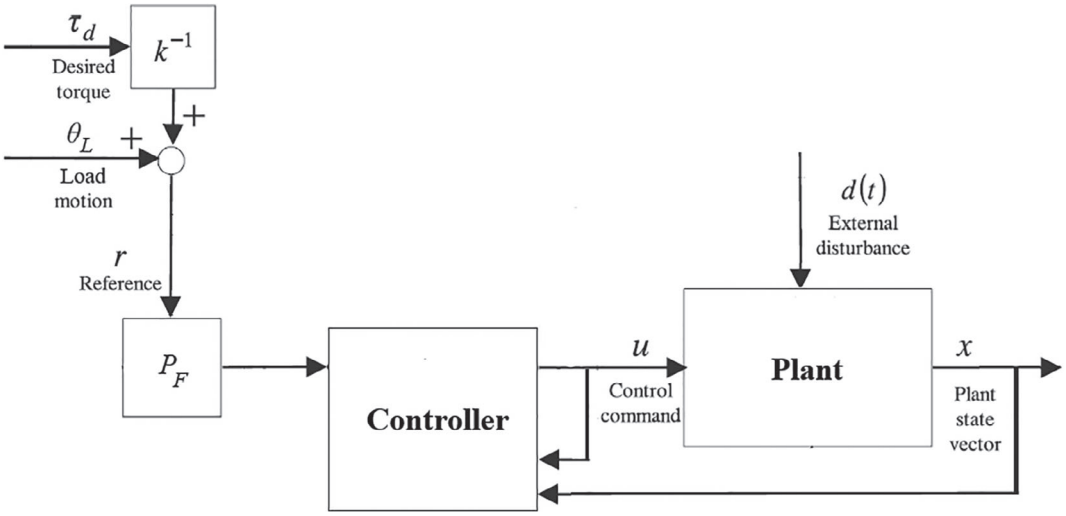

FIGURE 2 Block diagram of force control of an SEA

Step 2. By using observability, the ESO, which can estimate multiple lumped disturbances and their derivatives, is designed as in (20) and (38).

Step 3. A new reference signal with no steady-state error is generated by using (45) if needed.

5.1 | Force control

The block diagram of force control of an SEA is shown in Figure 2. P_F is a feedforward filter, that is

$$P_F = P_{n,\text{closed}} P_{\text{filter}} \tag{46}$$

where $P_{n,\text{closed}}$ is the inverse of the nominal closed-loop transfer function, P_{filter} is a low-pass filter to make the feedforward filter realizable. In the simulation, a sinusoidal external disturbance $4\sin(3t)$ Nm is applied to the load side all the time. The reference torque is set to zero and jumps to 1 Nm at the 3rd second in all following simulations. The control gain in (9) is set to $b = \frac{1}{I_M} = 190476$. The observer bandwidth of the conventional ADRC and the proposed ADRC both are chosen as $\omega_o = 40$ rad/s, which is much smaller than the observer bandwidth in Reference 25, because the order of observer is much smaller than that of observer in Reference 25. The control bandwidth is set to $\omega_c = 10$ rad/s as in Reference 20. The initial states of SEA in (1) and (2) are $x_0 = \begin{bmatrix} 0 & 0 & 0 & 0 \end{bmatrix}^T$. A second-order Butterworth filter is employed as the low-pass filter in (46) with cutoff bandwidth of 200 rad/s.

It is interesting to notice that the simulation results of time delay control proposed in Reference 20 do not converge when using the parameters in Table 1. This may be due to the reason that the ratio of load inertia to motor equivalent inertia and the ratio of load damping to motor equivalent damping are high, which are about 10.71 times and 258.89

times, respectively. Much model information is lost without considering any model information. Time delay is introduced into time delay control, which is undesirable in control design. This may cause unstable. The performance of time delay control is not very good as mentioned in Reference 21. Moreover, Reference 20 does not provide any system parameters to verify the performance of time delay control.

Like the time delay control proposed in Reference 20, conventional LADRC does not need any model information except the relative degree of the system. To improve the control performance, the known model information and two output measurements are incorporated into ADRC design in this paper. Figure 3 shows the force control results when the conventional ADRC and the proposal ADRC design are simulated. The corresponding interaction force is calculated by $k\left(\frac{x_M}{N} - x_L\right)$. The control signals are given in Figure 4. As shown in Figure 4, the control signal of conventional ADRC slightly lags behind that of proposed ADRC, which causes an oscillation when reference force trajectory jumps to 1 Nm at the 3rd second, because more model information is incorporated into proposed ADRC. Moreover, the performance of disturbance rejection is limited by the cutoff frequency of the low pass filter. Increasing cutoff frequency will greatly decrease the oscillation caused by external disturbance at load side. But it will generate a larger spike when the reference jumps at the 3rd second. Figure 5 shows that the proposed ADRC has the ability to estimate the external disturbance although the estimated disturbance is a little lag behind the actual disturbance. This lag can be alleviated by increasing observer bandwidth.

Robust force control of SEAs proposed in Reference 22 also utilizes nominal model information, but DOB is used to estimate the total disturbance and compensate it. For comparing the proposed ADRC and DOB, the feedback gains of PD controller in Reference 22 are not set by linear quadratic (LQ) method but pole placement, that is, control bandwidth of

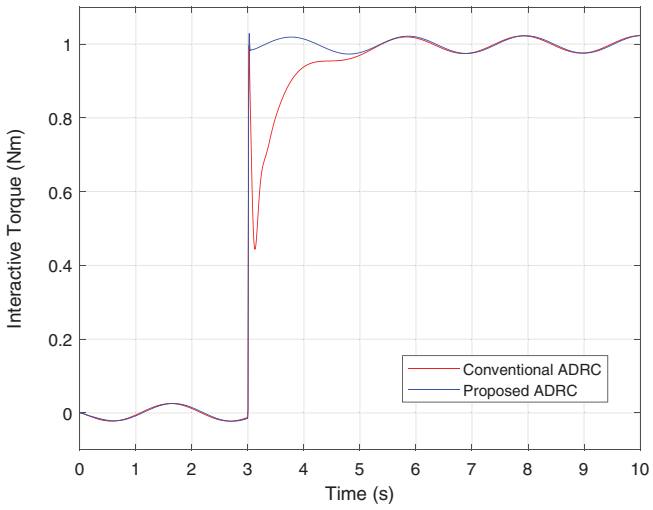

FIGURE 3 Simulation results of interactive torque between motor side and load side

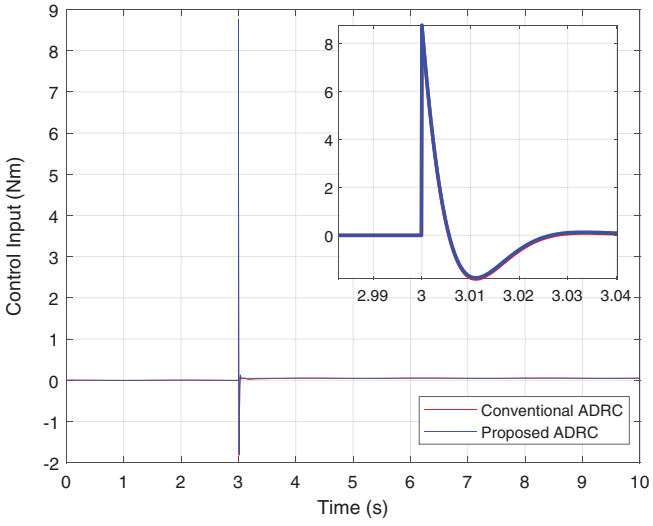

FIGURE 4 Control signals

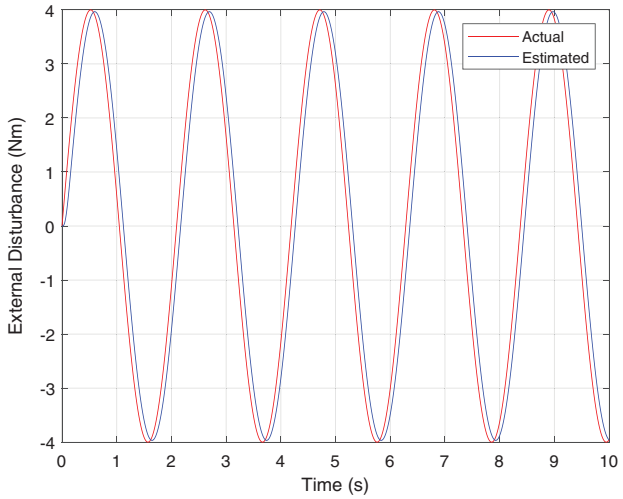

FIGURE 5 The external disturbance and its estimation

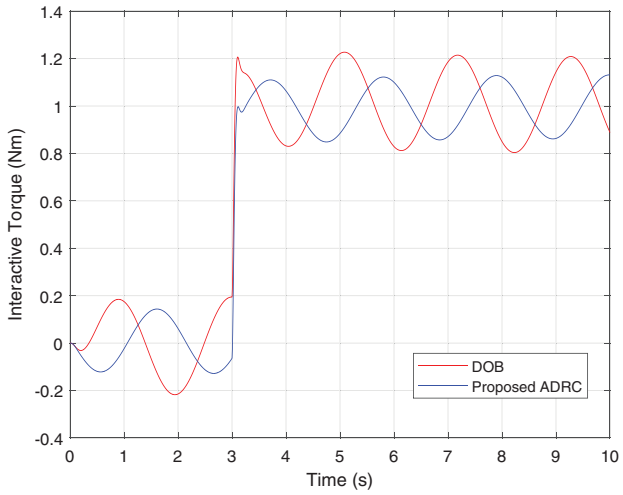

FIGURE 6 Simulation results of interactive torque between motor side and load side

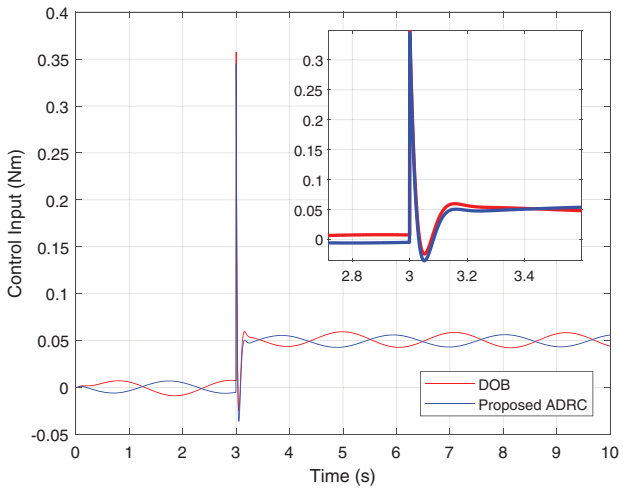

FIGURE 7 Control signals

10 rad/s. The cutoff frequency of the Q-filter in DOB is set to 40 rad/s. Moreover, the cutoff bandwidth of the low-pass filter in (46) is set to 40 rad/s, because the disturbance cannot be fully eliminated if the bandwidths of the Q-filter and the low-pass filter are not the same. Figure 6 shows the force control results of the DOB and the proposal ADRC. The control signals are shown in Figure 7. The interaction force of DOB is higher than that of proposed ADRC. This may be due to the reason that the proposed ADRC can fully decouple the motor side and load side and minimize the effect from external disturbance at load side.

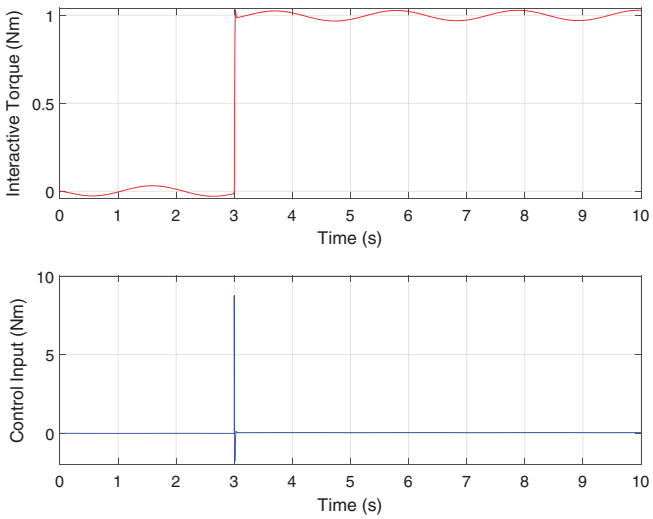

FIGURE 8 Simulation results of interactive torque between motor side and load side and control input

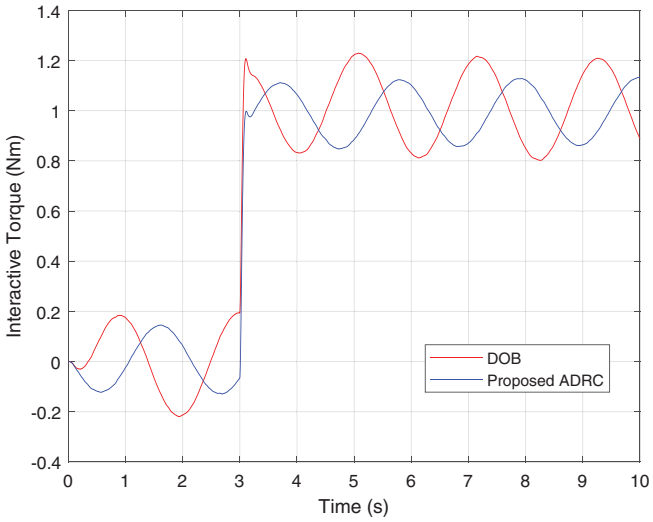

FIGURE 9 Simulation results of interactive torque between motor side and load side

To test the robustness of the proposed ADRC method, assume some parameters of the plant are unknown in the following simulation. The parameter of load inertia in the algorithm is set to 2.25 kg m^2, which is 100 times of its actual value 0.0225 kg m^2. The cutoff bandwidth of the low-pass filter is set to 200 rad/s. The corresponding interaction force between motor and load and control input are shown in Figure 8.

To test how noise affects the performances of the proposed ADRC and DOB, white Gaussian noises with mean zero and standard deviation 1.14 degrees are added into motor and load output measurements. Figure 9 shows the force control results of DOB and proposal ADRC. The control signals are shown in Figure 10. They have similar noise in the control signals, but the performance of proposed ADRC is still better than that of DOB.

5.2 | Position control

To illustrate the performance of the proposed ADRC design compared with extension of LADRC with entire model information, step reference input is applied in position control of a SEA. A step reference input of 1 rad is applied at 1 s. After plant reaches steady state, a step external disturbance of 1 Nm is applied at load side at 5 s. The control gain in (28) is set to $b = k/I_H I_M N = 203174$. The observer bandwidth and control bandwidth in all methods are chosen as $\omega_o = 40$ rad/s and $\omega_c = 20$ rad/s, respectively. The initial states of the SEA are $x_0 = \begin{bmatrix} 0 & 0 & 0 & 0 \end{bmatrix}^T$.

Let us first consider the nominal situation. To compensate for the mismatched disturbance, the disturbance at load side and its first- and second-order derivatives should be estimated. In the simulation, we found the first- and second-order

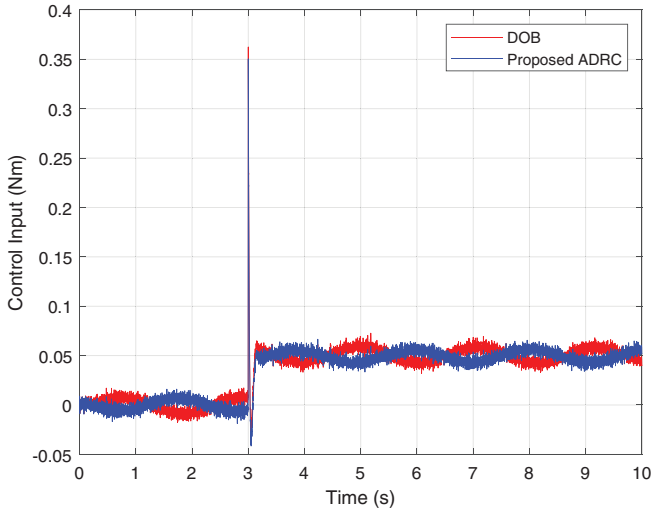

FIGURE 10 Control signals

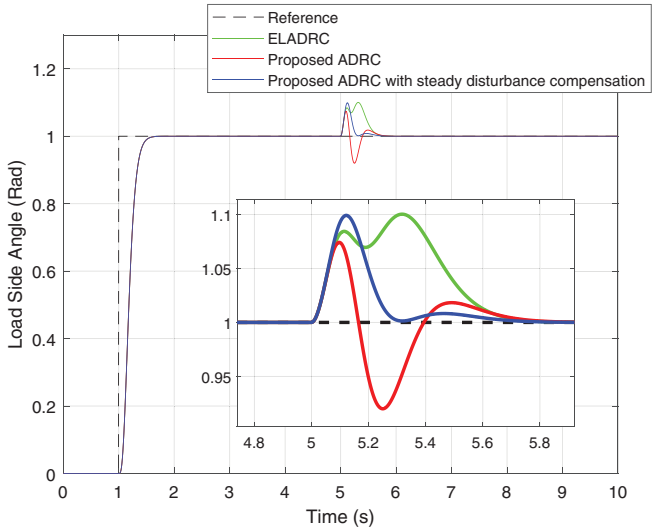

FIGURE 11 Simulation results of position control at load side

derivatives are slightly larger than their actual values if the external disturbance is sinusoidal, which may exaggerate the influence of change rate of disturbance and cause oscillation. Therefore, we set the first- and second-order derivatives both to zero that is to only compensate for disturbance in steady state. Figure 11 shows the simulation results of angle at load side. These three methods have similar trajectories in transient. When an external disturbance is applied at 5 s, these three methods show different performances. Figure 11 shows proposed ADRC with steady disturbance compensation has least oscillation while the overshoot of proposed ADRC with steady disturbance compensation is the highest. In all cases, there is no steady-state error. Figure 12 shows control input of each method. Since controller does not need to compensate for the derivatives of external disturbance, proposed ADRC with steady disturbance compensation consumes least energy. Figure 13 shows that proposed ADRC has the ability to estimate the external disturbance after discontinuous point of the disturbance, and it converges quickly. The spike in Figure 13 is caused by the higher-order DOB, that is, the extra two fictitious states in (38) to estimate the first- and second-order derivatives, which has been studied in Reference 42.

To test the robustness of these three methods, assume some parameters of the plant are unknown in the following simulations. The parameter of load inertia in the algorithm is doubled, which is set to 0.045 kg m^2, while the actual plant still uses its original value, which is 0.0225 kg m^2. Figure 14 shows the simulation results of angle at load side. Since the first- and second-order derivatives estimated in proposed ADRC are not accurate, the simulation result using proposed ADRC does not converge. So, simulation results of proposed ADRC with steady disturbance compensation and extended LADRC are shown in the following figures. As shown in Figure 14, proposed ADRC with steady disturbance compensation has much less oscillation in the transient response and at the time when an external disturbance is applied to load side. The trajectory details are shown in Figure 15. In both cases, there is no steady-state error.

FIGURE 12 Control signals

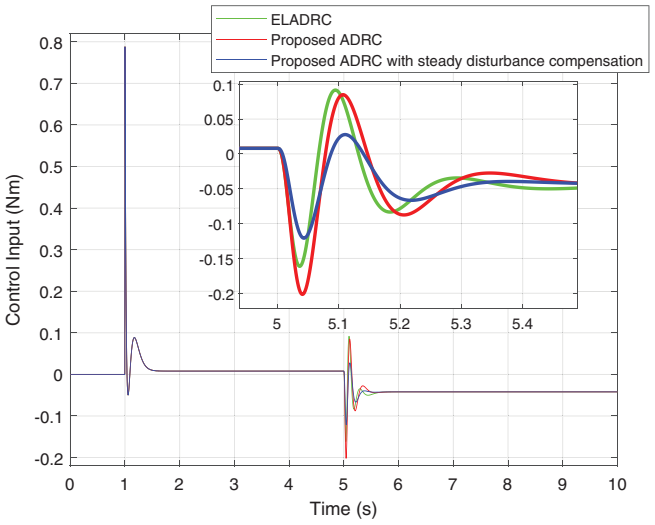

FIGURE 13 The external disturbance and its estimation

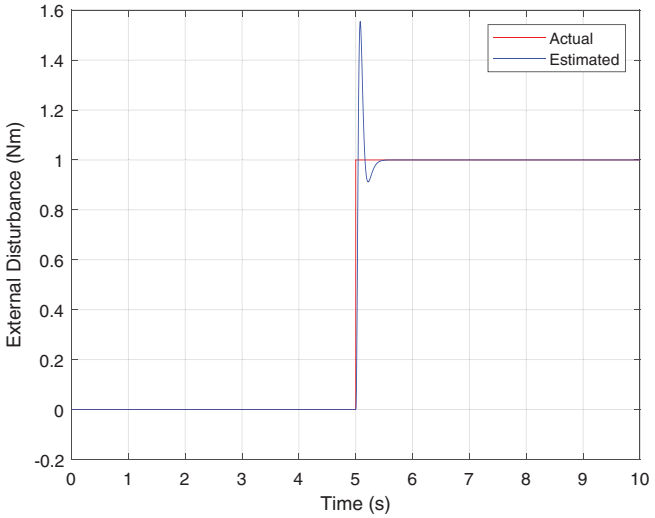

FIGURE 14 Simulation results of position control at load side

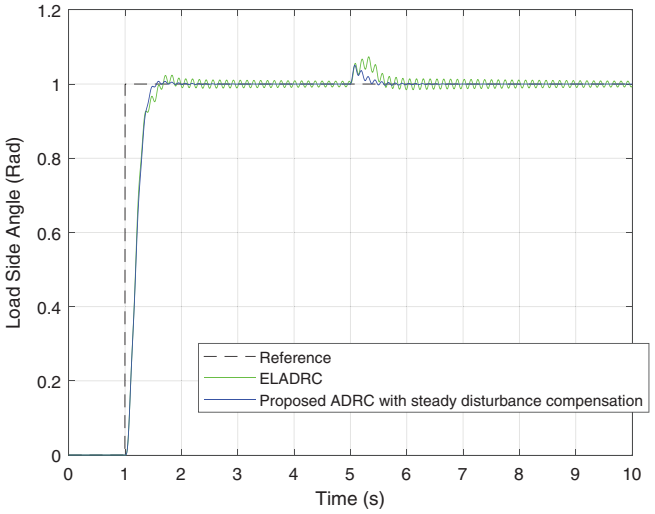

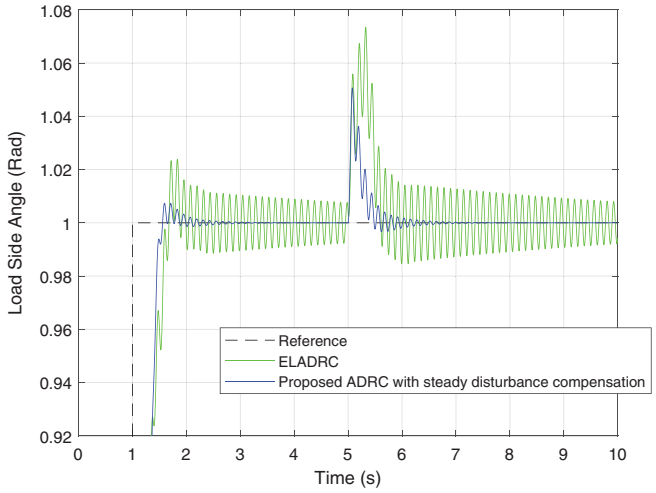

FIGURE 15 Trajectory details of position control at load side

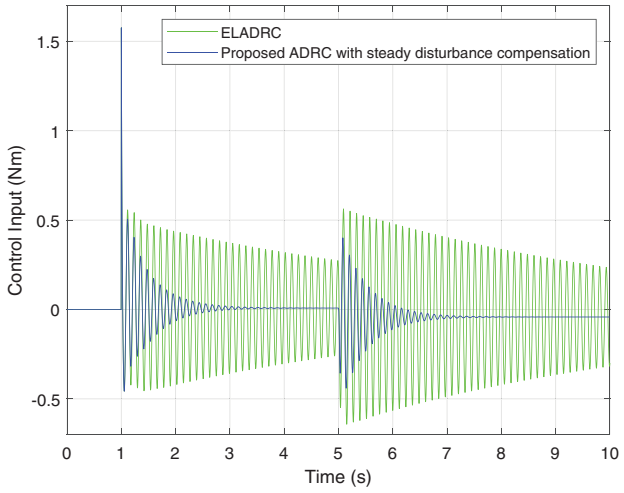

FIGURE 16 Control signals

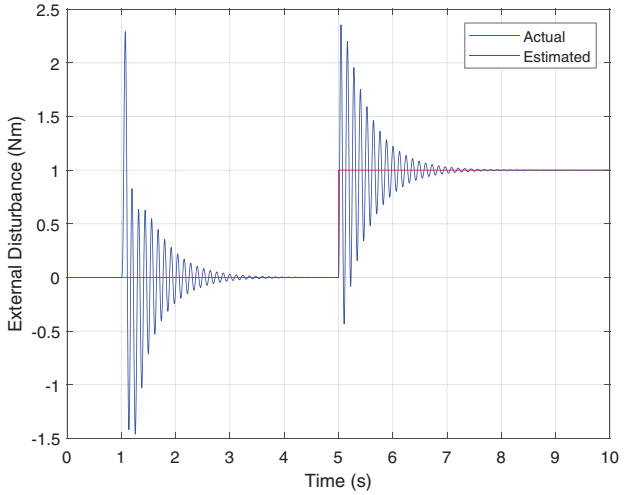

FIGURE 17 The external disturbance and its estimation

Figure 16 shows control signals of these two methods. Proposed ADRC with steady disturbance compensation consumes much less energy like the nominal case. Figure 17 shows the actual external disturbance and its estimation. Even if the plant model is not very accurate, proposed ADRC still can get accurate estimation after discontinuous point of the disturbance.

To test how noise affects the performance of the proposed ADRC method and ELADRC, white Gaussian noises with mean zero and standard deviation 1.14 degrees are added into motor and load output measurements. Since parameters of SEA is designed for force control,[24] the spring between motor side and load side is very soft, which makes the SEA system

FIGURE 18 Simulation results of position control at load side

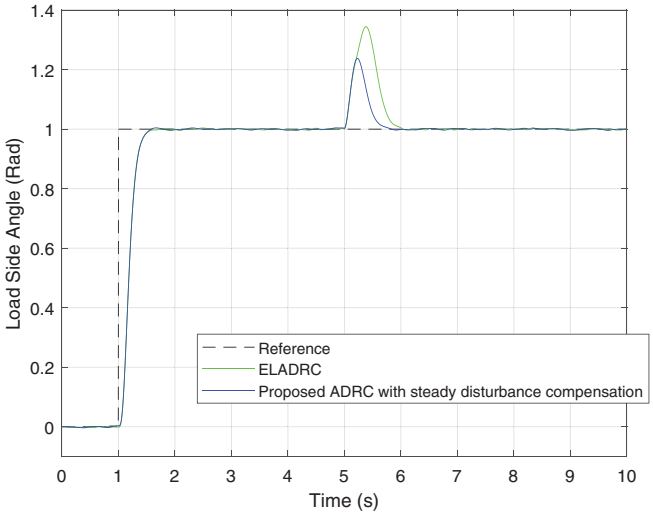

FIGURE 19 Control signals

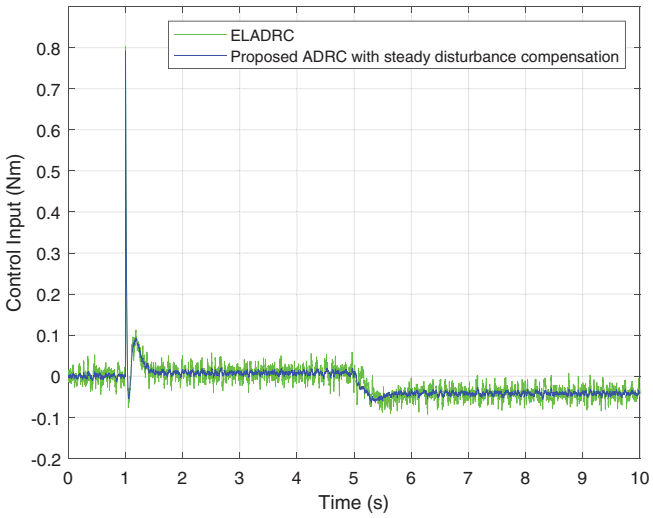

very sensitive to noise in position control mode. The observer bandwidth is changed to 20 rad/s in this noise simulation. Moreover, in ESO design, only two lumped disturbances at motor side and load side are estimated to implement proposed ADRC with steady disturbance compensation. Figure 18 shows the simulation results of angle at load side. The control signals are shown in Figure 19. As shown in these two figures, the overshoot of proposed ADRC with steady disturbance compensation is lower than that of ELADRC. Moreover, the noise in control signal is much less than that of ELADRC.

6 | CONCLUSION

In this paper, the full methodology of ADRC design is utilized to address the robust force and position control problems of SEAs with model uncertainty and exogenous disturbance. Since ADRC is formulated in the language of state space description, various model and measurements information can be readily incorporated into the design. On the one hand, ADRC-based design can be made very simple, based on only the relative degree of the plant. It also can incorporate entire known model information and all measurable outputs. Such flexibility allows the often under-appreciated trade-off between performance and bandwidth. In particular, for the SEAs, incorporating the known model information and both angular measurements the ADRC design will lessen the burden of ESO, allowing high performance at lower bandwidth.

Regarding the multiple disturbances in SEAs, the observability and controllability in the framework of modern control theory can be generalized to cases which include not only plant states but also lumped disturbances in all channels. In this research, we find that the observability and controllability are very important concepts in ADRC design and should be fully used.

The simulations have validated the conceptual design in which the robustness and performance of the proposed design are better than those based on the conventional LADRC, extension LADRC, time delay control and DOB. And the observer bandwidth of ESO is very low compared to the unified ADR motion controller combining differential flatness and DOB in state space. In a nutshell, we now have a fully implementable ADRC solution for the SEAs.

CONFLICT OF INTEREST

The authors declare no potential conflict of interest.

DATA AVAILABILITY STATEMENT

Data sharing not applicable to this article as no datasets were generated or analysed during the current study.

ORCID

Jinfeng Chen https://orcid.org/0000-0002-9375-2548

REFERENCES

1. Yan T, Cempini M, Oddo CM, Vitiello N. Review of assistive strategies in powered lower-limb orthoses and exoskeletons. Robot Autonom Syst. 2015;64:120-136.
2. Yu H, Huang S, Chen G, Pan Y, Guo Z. Human–robot interaction control of rehabilitation robots with series elastic actuators. IEEE Trans Robot. 2015;31(5):1089-1100.
3. Wang S, Wang L, Meijneke C, et al. Design and control of the MINDWALKER exoskeleton. IEEE Trans Neural Syst Rehab Eng. 2015;23(2):277-286.
4. Blaya JA, Herr H. Adaptive control of a variable-impedance ankle-foot orthosis to assist drop-foot gait. IEEE Trans Neural Syst Rehab Eng. 2004;12(1):24-31.
5. Matt C, Shu T, Stolyarov R, Duval JF, Herr H. Design and preliminary results of a reaction force series elastic actuator for bionic ankle prostheses; 2019. engrXiv.
6. Paine N, Mehling JS, Holley J, et al. Actuator control for the NASA-JSC Valkyrie humanoid robot: a decoupled dynamics approach for torque control of series elastic robots. J Field Robot. 2015;32:378-396.
7. Knabe C, et al. Design of a series elastic humanoid for the DARPA Robotics Challenge. Paper presented at: 2015 IEEE-RAS 15th International Conference on Humanoid Robots (Humanoids), Seoul; 2015:738–743.
8. Pratt GA, Williamson MM. Series elastic actuators. Paper presented at: Proc. 1995 IEEE/RSJ Int. Conf. Intelligent Robots and Systems; 1995; Pittsburgh, PA:399–406.
9. Vanderborght B, Albu-Schaeffer A, Bicchi A, et al. Variable impedance actuators: a review. Robot Autonom Syst. 2013;61(12):1601-1614.
10. Sun W, Zhao Y, Li J, Zhang L, Gao H. Active suspension control with frequency band constraints and actuator input delay. IEEE Trans Indus Electron. 2012;59(1):530-537.
11. Li X, Zhou W, Luo J, et al. A new mechanical resonance suppression method for large optical telescope by using nonlinear active disturbance rejection control. IEEE Access. 2019;7:94400-94414.
12. Zhao S, Gao Z. An active disturbance rejection based approach to vibration suppression in two-inertia systems. Asian J Control. 2013;15(2):350-362.
13. Zhang H, Zhao S, Gao Z. An active disturbance rejection control solution for the two-mass-spring benchmark problem. Paper presented at: American Control Conference (ACC); 2016; Boston, MA:1566–1571.
14. Yun JN, Su J, Kim YI, Kim YC. Robust disturbance observer for two-inertia system. IEEE Trans Indus Electron. 2013;60(7):2700-2710.
15. Hori Y. A review of torsional vibration control methods and a proposal of disturbance observer-based new techniques. Paper presented at: Proc. 13th IFAC World Congr.; 1996.
16. Katsura S, Ohnishi K. Force Servoing by flexible manipulator based on resonance ratio control. IEEE Trans Indus Electron. 2007;54(1):539-547.
17. Vallery H, Veneman J, van Asseldonk E, Ekkelenkamp R, Buss M, van der Kooij H. Compliant actuation of rehabilitation robots. IEEE Robot Automat Mag. 2008;15(3):60-69.
18. Bae J, Kong K, Tomizuka M. Gait phase-based control for a rotary series elastic actuator assisting the knee joint. ASME. J Med Devices. 2011;5(3):031010.
19. Pratt J, Krupp B, Morse C. Series elastic actuators for high fidelity force control. Indus Robot. 2002;29(3):234-241.
20. Kim S, Bae J. Force-mode control of rotary series elastic actuators in a lower extremity exoskeleton using model-inverse time delay control. IEEE/ASME Trans Mechatronics. 2017;22(3):1392-1400.
21. Qing CZ, Alon K, Stobart RK. Design of UDE-based controllers from their two-degree-of-freedom nature. Int J Robust Nonlinear Control. 2010;17(21):1994-2008.
22. Kong K, Bae J, Tomizuka M. Control of rotary series elastic actuator for ideal force-mode actuation in human-robot interaction applications. IEEE/ASME Trans Mechatronics. 2009;14(1):105-118.
23. Paine N, Oh S, Sentis L. Design and control considerations for high-performance series elastic actuators. IEEE/ASME Trans Mechatronics. 2014;19(3):1080-1091.

24. Oh S, Kong K. High-precision robust force control of a series elastic actuator. IEEE/ASME Trans Mechatronics. 2017;22(1):71-80.
25. Sariyildiz E, Chen G, Yu H. A unified robust motion controller design for series elastic actuators. IEEE/ASME Trans Mechatronics. 2017;22(5):2229-2240.
26. Sariyildiz E, Mutlu R, Zhang C. Active disturbance rejection based robust trajectory tracking controller design in state space. J Dyn Syst Meas Control. 2019;141(6):061013.
27. Sariyildiz E, Chen G, Yu H. An acceleration-based robust motion controller design for a novel series elastic actuator. IEEE Trans Indus Electron. 2016;63(3):1900-1910.
28. Tomei P. A simple PD controller for robots with elastic joints. IEEE Trans Automat Control. 1991;36(10):1208-1213.
29. Luca AD, Siciliano B, Zollo L. PD control with on-line gravity compensation for robots with elastic joints: theory and experiments. Automatica. 2005;41(10):1809-1819.
30. Zhao W, Sun L, Yin W, Li M, Liu J. Robust position control of series elastic actuator with backstepping based on disturbance observer. Paper presented at: IEEE/ASME International Conference on Advanced Intelligent Mechatronics (AIM); 2019; Hong Kong, China:618–623.
31. Chen S, Bai W, Hu Y, Huang Y, Gao Z. On the conceptualization of total disturbance and its profound implications. Sci China Inf Sci. 2020;63:129201.
32. Li S, Yang J, Chen W, Chen X. Generalized extended state observer based control for systems with mismatched uncertainties. IEEE Trans Indus Electron. 2012;59(12):4792-4802.
33. Bai W, Chen S, Huang Y, Guo BZ, Wu ZH. Observers and observability for uncertain nonlinear systems: a necessary and sufficient condition. Int J Robust Nonlinear Control. 2019;29:2960-2977.
34. Castillo A, García P, Sanz R, Albertos P. Enhanced extended state observer-based control for systems with mismatched uncertainties and disturbances. ISA Trans. 2018;73:1-10.
35. Han J. From PID to active disturbance rejection control. IEEE Trans Ind Electron. 2009;56(3):900-906.
36. Gao Z. Scaling and bandwidth-parameterization based controller tuning. Paper presented at: Proc. 2003 Amer. Control Conf.; 2003; Denver, CO:4989–4996.
37. Tan W, Fu C. Linear active disturbance-rejection control: analysis and tuning via IMC. IEEE Trans Indus Electron. 2016;63(4):2350-2359.
38. Fu C, Tan W. Tuning of linear ADRC with known plant information. ISA Trans. 2016;65(11):384-393.
39. Yang J, Chen WH, Li S, Chen X. Static disturbance-to-output decoupling for nonlinear systems with arbitrary disturbance relative degree. Int J Robust Nonlinear Control. 2013;23(5):562-577.
40. Dorf RC, Bishop RH. Modern Control System. 12th ed. Upper Saddle River, NJ: Prentice Hall; 2011.
41. Sira-Ramirez H, Oliver-Salazar MA. On the robust control of Buck-converter DC-motor combinations. IEEE Trans Power Electron. 2013;28(8):3912-3922.
42. Madoński R, Herman P. On the usefulness of higher-order disturbance observers in real control scenarios based on perturbation estimation and mitigation. Paper presented at: 9th International Workshop on Robot Motion and Control; 2013; Kuslin:252–257.

How to cite this article: Chen J, Hu Y, Gao Z. On practical solutions of series elastic actuator control in the context of active disturbance rejection. *Advanced Control for Applications: Engineering and Industrial Systems*. 2021;3:e69. https://doi.org/10.1002/adc2.69